HHS Public Access

Author manuscript

J Vis Exp. Author manuscript; available in PMC 2024 February 17.

Using *Ex Vivo* Live Imaging to Investigate Cell Divisions and Movements During Mouse Dental Renewal

Abinaya Sundari Thooyamani[1,†], **Elias Shahin**[2,†], **Sanako Takano**[1], **Amnon Sharir**[2,*], **Jimmy K. Hu**[1,3,*]

[1]School of Dentistry, University of California Los Angeles, Los Angeles, CA, USA

[2]The Institute of Biomedical and Oral Research, Faculty of Dental Medicine, Hebrew University of Jerusalem, Jerusalem, Israel

[3]Molecular Biology Institute, University of California Los Angeles, Los Angeles, CA, USA

Abstract

The continuously growing mouse incisor is emerging as a highly tractable model system to investigate the regulation of adult epithelial and mesenchymal stem cells and tooth regeneration. These progenitor populations actively divide, move, and differentiate in order to maintain tissue homeostasis and regenerate lost cells in a responsive manner. However, traditional analyses using fixed tissue sections could not capture the dynamic processes of cellular movements and interactions, limiting our ability to study their regulations. This paper describes a protocol to maintain whole mouse incisors in an explant culture system and live track dental epithelial cells using multiphoton timelapse microscopy. This technique adds to our existing toolbox for dental research and allows investigators to acquire spatiotemporal information of cell behaviors and organizations in a living tissue. We anticipate that this methodology will help researchers further explore mechanisms that control the dynamic cellular processes taking place during both dental renewal and regeneration.

SUMMARY:

Ex vivo live imaging is a powerful technique for studying the dynamic processes of cellular movements and interactions in living tissues. Here, we present a protocol that implements two-photon microscopy to live track dental epithelial cells in cultured whole adult mouse incisors.

INTRODUCTION:

Over the past two decades, the mouse incisor has emerged as an invaluable platform for investigating the principles of adult stem cell regulation and tooth regeneration[1, 2]. The mouse incisor grows continuously and renews itself throughout the animal's life. It does

*Corresponding authors: Jimmy K. Hu jkhu@ucla.edu; Amnon Sharir amnon.sharir@mail.huji.ac.il.
†These authors contributed equally.

A complete version of this article that includes the video component is available at http://dx.doi.org/10.3791/66020.

DISCLOSURES:
The authors have no conflicts of interest to disclose.

so by maintaining both epithelial and mesenchymal stem cells, which can self-renew and differentiate into different cell types of the tooth[1, 2]. While dental epithelial stem cells give rise to ameloblasts, which secrete the enamel matrix, dental mesenchymal stem cells give rise to odontoblasts, cementoblasts, and fibroblasts, which form dentin, cementum, and periodontal ligament, respectively[3–6]. This constant supply of new cells maintains tissue homeostasis and allows the replacement of old cells that are lost due to masticatory wear or injuries[7, 8]. Elucidating the cellular and molecular mechanisms that regulate the maintenance and differentiation of dental stem cells is therefore central to understanding dental regeneration, an area of growing interest.

Anatomically, a large portion of the adult mouse incisor is encased in the jawbone. While the incisal edge of the tooth is exposed, the apical end of the incisor fits within a socket and is firmly attached to the surrounding bone through periodontal ligaments and connective tissues (Figure 1A,B). The incisor apical end is also the growth region of the tooth and maintains dental stem and progenitor cells in both the epithelial layer and the mesenchymal pulp[9–13]. Specifically, dental epithelial stem cells are maintained at the bulbous end of the epithelium, known as the apical bud, also referred to as the labial cervical loop (Figure 1C). Similar to the intestinal epithelium and the epidermis, epithelial renewal in the incisor is primarily supported by actively cycling stem cells and their highly proliferative intermediate descendants, called transit-amplifying cells[14–17], both residing in the inner part of the cervical loop. However, whether the incisor epithelium contains and utilizes quiescent stem cells during regeneration remains to be determined. In contrast, both active and quiescent dental mesenchymal stem cells have been identified in the apical pulp, and the quiescent stem cells function as a reserve population that becomes activated during injury repair[13, 18].

Many of the discoveries on the biology of the mouse incisor renewal and regeneration have resulted from histological investigations, in which samples are obtained at distinct temporal junctures, fixed, processed, and then sectioned into micron-thin slices along a particular plane. Through detailed analysis of histological sections from different mouse models that enable lineage tracing or genetic perturbations, scientists have identified the cell lineages of different progenitor populations, as well as the genetic and signaling pathways that control incisor homeostasis and injury repair[19–21]. However, the static two-dimensional (2D) images of non-vital cells in sections cannot capture the full spectrum of cellular behaviors and spatial organizations in a living tissue, such as cell shape changes, movements, and cellular kinetics. Detecting and measuring these rapid cellular changes, which occur at a timescale that is unresolvable through tissue sectioning, require a different strategy. Moreover, acquiring such information is also critical for understanding how dental cells interact with each other, react to different signaling stimuli, and self-organize to maintain tissue structures and functions.

The advent of four-dimensional (4D) deep tissue imaging using two-photon microscopy[22], a technology that integrates three spatial dimensions with temporal resolution, overcomes the inherent limitations of histological analysis by enabling spatiotemporal examination of cultured tissue explants, organoids, or even tissues *in situ*[23–26]. For instance, 4D live imaging of the developing tooth epithelium has unveiled the spatiotemporal patterns of cell divisions and migrations that coordinate tissue growth, signaling center formation,

and dental epithelial morphogenesis[27–32]. In the adult mouse incisor, 4D imaging has been recently adapted to study cellular behaviors during dental epithelial injury repair. Live imaging revealed that stratum intermedium cells in the suprabasal layer can be directly converted into ameloblasts in the basal layer to regenerate the damaged epithelium, challenging the traditional paradigm of epithelial injury repair[15].

Here, we describe the dissection, culturing, and imaging of the adult mouse incisor, focusing on epithelial cells in the labial cervical loop (Figure 1). This technique preserves dental cell vitality for more than 12 h and permits live tracking of fluorescently labeled cells at single-cell resolution. This approach allows investigation of cell motion and migration as well as dynamic changes in cell shape and division orientation under normal culture conditions, or in responses to genetic, physical, and chemical perturbations.

PROTOCOL:

All mice were maintained in pathogen-free animal facilities at the University of California Los Angeles (UCLA) or Hebrew University of Jerusalem (HUJI). All experiments involving mice were performed according to regulations and protocols approved by the respective Institutional Animal Care and Use Committee (IACUC) (ARC-2019-013; UCLA) or (MD-23-17184-3; HUJI). A general workflow of the experimental steps is shown in Figure 2A. See the Table of Materials for details related to all instruments, reagents, and materials used in this protocol.

1. Preparation of solutions and gels

1.1. Dissection medium: Prepare fresh DMEM/F12 with 0.5% glucose and keep it warm at 37 °C until needed in step 2.4.

NOTE: We use DMEM/F12 without phenol red to reduce autofluorescence during live imaging.

1.2. 1x Culture medium: Prepare fresh medium using 50% DMEM/F12, 50% rat serum, 1x glutamine substitute, 1x MEM Non-Essential Amino Acids, 1% glucose, 0.1 mg/mL L-ascorbic acid, and 0.5% penicillin-streptomycin. Keep it warm at 37 °C until needed in step 5.5. This medium is used for culturing incisor explants during live imaging.

NOTE: The rat serum should be of high quality and specially prepared for whole tissue culturing by researchers or from a commercial source. In particular, the blood must be centrifuged (5 min at 1200 g for 5 min at room temperature) before clotting begins to form. After centrifugation, the resulting fibrin clot should be squeezed and discarded[33].

1.3. Culture gel: The purpose of the gel is to immobilize samples during imaging and is prepared fresh.

1.3.1. Make 2% gel in DMEM/F12 by dissolving 200 mg of low melting point agarose in 10 mL of DMEM/F12 using a microwave. Keep the 2% gel at 37 °C.

1.3.2. Make 2x culture medium (without DMEM/F12) by mixing 50% rat serum, 1x glutamine substitute, 1x MEM Non-Essential Amino Acids, 1% glucose, 0.1 mg/mL L-ascorbic acid, and 0.5% penicillin-streptomycin. Warm the 2x culture medium (without DMEM/F12) to 37 °C.

1.3.3. Make 1% culture gel by mixing equal volumes of 2% gel and 2x culture medium (without DMEM/F12). Keep the 1% culture gel at 37 °C until needed in step 5.1.

NOTE: Make sure all solutions are warm before mixing to avoid gelling. We found 1% gel to be suitable for culturing the adult mouse incisor. Gel percentage should be empirically determined if other tissues are to be cultured.

2. Extraction of the adult mouse mandibles

2.1. Euthanize mice at the desired age using standard procedures approved by the IACUC.

NOTE: Here we use CO_2 asphyxiation followed by cervical dislocation. Regulations for animal euthanasia may vary in different regions. Researchers should obtain necessary institutional approval prior to performing experiments and ensure compliance with local animal care regulations.

2.2. Disinfect the mouse using 70% ethanol.

2.3. Decapitate the mouse and extract the left and right mandibles.

2.3.1. Lay the mouse on its belly, then use a #9 single edge industrial razor blade to cut at the neck region and separate the mouse head from the rest of the body.

NOTE: If tissues from the pharynx or the neck region are to be collected as well, decapitation should not be performed, and one can directly proceed to step 2.3.2.

2.3.2. Turn the mouse over so its ventral side is facing up and the mandibles are easily accessible.

2.3.3. Secure the animal’s head by holding it gently between the thumb and the index finger.

2.3.4. Use the razor blade to make a mid-sagittal incision that cuts over the skin of the lower jaw from the lower lip towards the neckline.

NOTE: A #15 surgical blade can also be used to make the incision and subsequent dissections (steps 2.3.6–2.3.9).

2.3.5. As the incision is made, spread open the cut skin using the thumb and the index finger to expose the muscles and jawbone underneath.

2.3.6. Use the razor blade to sever the masseter muscles on the buccal side of the lower jaw, such that the outside of the left and right hemimandibles are now free from muscle attachments.

2.3.7. Sever the mylohyoid muscles along the inner side of the mandible to remove muscle attachments there.

2.3.8. Make another incision at the mandibular symphysis that connects the two hemimandibles. Once cut, the mandible will be separated into the left and right halves.

2.3.9. Wedge the razor blade between the mandibular condyle and the temporal mandibular joint and carefully dissect out the hemimandible from the rest of the head.

NOTE: We found it helpful to simultaneously pull gently on the incisor while cutting. Care should be taken to avoid breaking the mandible and damaging the soft tissues within.

2.4. Immediately transfer dissected mandibles to a Petri dish with the prewarmed dissection media (step 1.1) and remove the remaining muscle tissues using a #15 surgical blade.

NOTE: Keeping samples in cold media slows down cell activities, resulting in delayed or even failed recoveries of certain cell activities, such as proliferation or cell movement, during live imaging.

3. Isolation of the whole mouse incisors

NOTE: Further isolation of the incisor is done under a bright field dissection microscope.

3.1. Visually identify the oval region of the mandible that covers the incisor socket and houses the apical portion of the incisor.

3.2. Position the mandible so the inner (lingual) surface is facing upwards.

3.3. While holding the mandible in place with a pair of serrated forceps, generate a window at the oval region by shaving off the overlying membrane bone using a #15 surgical blade, in a direction that is from the condyle towards the molars. This exposes the soft tissue of the apical incisor on the inner surface.

3.4. Turn over the mandible so the outer (buccal) surface is facing upwards.

3.5. Generate a window at the oval region on the outer mandible as described in step 3.4 and use the tip of the scalpel to pick away any remaining bone fragments at the edge. Ensure that the apical end of the tooth is visible from both sides.

NOTE: Avoid excessive pressure while shaving the bones to prevent damage to the underlying soft tissue.

3.6. Systematically cut away the bones surrounding the incisor to isolate the entire tooth.

3.6.1 Make a clean cut at a plane that is immediately adjacent to the apical incisor to first remove the condylar process.

NOTE: Be careful not to cut into the incisor.

3.6.2. Make a second cut just posterior to the 3rd molar, but dorsal to the incisor without damaging the tooth. This removes the bone that includes the coronoid process.

3.6.3. Serially cut from the tip of the angular process towards the incisor to gradually remove the ventral mandible in a stepwise manner.

NOTE: The dental epithelium and associated periodontal tissues are often stuck to the bone and easily ripped off if a large portion of the ventral bone is cut at once. To separate the bone from the incisor soft tissue, one can insert the scalpel (or a pair of sharp non-serrated forceps) between the two tissues at the apical end of the incisor and delicately slide the instrument forward.

3.6.4. Cut away the alveolar bone with molars and any remaining bones that are still attached to the incisor.

3.6.5. The entire incisor is now isolated. Transfer the fully dissected incisor to a dish with clean warm dissection media (step 1.1).

3.7. Repeat steps 3.2–3.7 to isolate additional incisors as required.

NOTE: The maxillary/upper incisors of the mouse also maintain adult stem cells and can be used to study tooth regeneration[34]. Dental researchers typically focus on the lower incisors because they are more accessible and can be more easily dissected than the upper incisors. Differences between mandibular and maxillary incisor progenitor cells remain to be determined.

4. Removal of periodontal tissues to expose the incisor epithelial cervical loop

4.1. With the whole incisor lying down on its lingual side and while holding the tooth in place with a pair of serrated forceps, use a pair of #5 fine forceps to start tucking on the periodontal tissues covering the apical incisor and the cervical loop region.

4.2. Carefully peel off the periodontal tissue from the apical bud, such that the lateral side of the cervical loop (or other regions of interests) becomes clearly visible under the scope.

NOTE: Care should be taken to avoid damaging the dental epithelium or detaching it from the mesenchyme. If the incisor has fluorescence signals in the region of interest, and a fluorescent dissection microscope is available, fluorescence signals can be used to help distinguish between tissue types and aid dissections. It is important to efficiently carry out sections 2–4 so samples can be quickly transferred into the culture media and adequately maintained through explant culturing (see below).

5. Tissue embedding for explant culture

5.1. Add 500 μL of warm, unsolidified culture gel to a well in a 24-well plate and quickly transfer the dissected whole incisors to the well. Swirl the plate a few times to rinse the incisors.

5.2. Add 400 μL of warm, unsolidified culture gel to a culture dish and transfer the rinsed incisors to the dish.

NOTE: We use a commercially available culture dish from Bioptechs that is compatible with the Bioptech perfusion setup. See 6.4 for alternative options.

5.3. Orient the incisor to position the cervical loop region (or other regions of interests) at the center of the dish (Figure 2A,B) and adjust the tilt of the apical incisor for the desired imaging plane.

NOTE: Tissue orientation should be done quickly before complete gelation.

5.4. After the gel is set, use a pair of fine forceps to remove any gel on top of the region of interest so it is not covered by gel.

5.5. Add a sufficient volume of warm culture media by slowly pipetting it against the edge of the dish to just cover the sample (~150 μL).

5.6 Move the explant culture to a 37 °C cell culture incubator to allow tissue settling and adjustment to the culture condition for 1 h.

6. Timelapse microscopy of incisor explants

NOTE: In this experiment, we used an upright microscope equipped with a 25x water dipping objective that has a numerical aperture of 1. In general, a water dipping lens with a high numerical aperture is best suited for deep tissue imaging.

6.1. Turn on the microscope and the two-photon laser.

6.2. Secure the culture dish to the stage adapter and mount the perfusion adapter ring on top (Figure 2C).

6.3. Connect the stage adapter to a temperature controller set to maintain the culture at 37 °C.

6.4. Connect the inlet and the outlet of the adapter ring to a micro-perfusion pump and begin perfusion of the culture medium, with the perfusion speed set at 20 on the pump. This generates a slow flow (~5 mL/h) of the culture medium over the top of the samples (Figure 2C).

NOTE: We use the Bioptechs Delta T system to maintain the tissue in a stably controlled environment. Other systems can be used as well. A combination of a 37 °C heating plate and a homemade perfusion culture dish (Supplemental Figure S1) with an inlet and an outlet connected to syringe pumps can also be used.

6.5. Place an Atmospheric Control Barrier Ring (ACBR) on top of the adapter ring and lower the objective through the ACBR to just make contact with the culture medium (Figure 2D).

6.6. Tune the laser wavelength to 920 nm to visualize both GFP and red fluorescence (e.g., tdTomato) signals.

6.7. Locate samples through eyepieces and then on the microscope's software.

6.8. Set up Z-stacks, multi-position imaging, and time intervals using the software. To follow this protocol, use a **z-step size** of **4 μm** and a **time interval** of **5 min** for **14 h**.

NOTE: We found that a time interval of longer than 5 min is often insufficient to capture smooth cell movements and divisions.

6.9. Initiate the timelapse imaging.

NOTE: Sample position may shift during the first hour and further adjustments may be required.

6.10. Save files for downstream data processing and analyses.

REPRESENTATIVE RESULTS:

The apical region of the adult mouse incisor is encased within the mandible (Figure 1) and hence, not directly accessible for visualizing and live-tracking the progenitor cells residing within the growth region. Therefore, we have developed a method to extract the whole incisor from the jawbone and maintain it in an explant culture system for two-photon timelapse microscopy (Figure 2). Here we describe representative results that capture the dynamic process of cell proliferation and movement in the labial cervical loop region of the dental epithelium.

To demonstrate the experimental procedures, we have used two different mouse models that express green fluorescence in the dental epithelium. The first mouse line is $K14^{Cre};R26^{rtTA};tetO\text{-}H2B\text{-}GFP$, where $K14^{Cre}$ (MGI:2680713) expresses the Cre recombinase from a Keratin 14 promoter[35] and activates the expression of the reverse tetracycline-controlled transactivator in the epithelium from the $R26^{rtTA}$ allele[36] (MGI:3584524). Upon administration of doxycycline, rtTA induces histone H2B-GFP expression from the *tetO-H2B-GFP* allele[37] (MGI:3043783) and labels epithelial cell nuclei with green fluorescence. This is especially useful for cell-tracking and for detecting cell divisions. In this experiment, we fed animals with doxycycline food for 24 h before sacrifice to activate H2B-GFP expression. The second mouse line is $K14^{Cre};R26^{mT/mG}$, in which $R26^{mT/mG}$ (MGI:3803814) is a Cre-reporter[38]. In the absence of Cre activity, cells express membrane-localized tdTomato (mT) with red fluorescence. Upon Cre-mediated recombination, cells express membrane GFP (mG). $K14^{Cre};R26^{mT/mG}$ thus labels epithelial cell membranes with green fluorescence, leaving non-epithelial cells red. This permits easy visualization of cell shapes, divisions, and movements.

We began the procedure by dissecting out the mandibles (Figure 3A) and then systematically removed all the bones surrounding the incisor (Figure 3B–G). This yielded whole incisors with undamaged epithelium (Figure 3H). We confirmed the intactness of the dental epithelium by inspecting the green fluorescence in the $K14^{Cre};R26^{rtTA};tetO\text{-}H2B\text{-}GFP$ and

K14^{Cre};*R26*$^{mT/mG}$ mice (Figure 4A,B,E,F). At this stage, the opaque periodontal tissues still cover the apical incisor, and the cervical loop thus appears blurry due to light scattering, which would similarly hinder downstream timelapse imaging (Figure 4C,G). We therefore carefully removed the periodontal tissues, so the dental epithelium with the cervical loop could be clearly discerned in each incisor (Figure 4D,H).

The incisors were then embedded in low melting point agarose and cultured in a perfusion setup for two-photon live imaging as depicted in Figure 2. For this exercise, we have focused on the cervical loop region of the dental epithelium and captured z-stack images at 4 μm intervals every 5 min over a duration of 14 h (Figure 5A). Notably, H2B-GFP signals were mostly observed in the transit-amplifying region of the cervical loop, where there are active cell divisions (Figure 5B). This is likely because there is higher H2B-GFP exchange at open chromatins and incorporation into nucleosomes following DNA replications in these active cells[39].

We subsequently examined the timelapse images using ImageJ and based on the separating of the H2B-GFP signals[40], we were able to observe numerous cell divisions throughout the imaging period (Supplemental Video S1 and Supplemental Video S2). This indicated that the tissues were adequately maintained in the explant culture and cells were active. Specifically, we were able to observe the condensation and alignment of chromosomes at the metaphase plate in mitotic cells, followed by their segregation into two daughter cells during anaphase (Figure 5C–N, manually tracked using the ImageJ plugin TrackMate). Most of these divisions were perpendicular or at an oblique angle relative to the basement membrane (Figure 5C–K and Supplemental Video S1). Horizontal divisions parallel to the basement membrane could also be detected, although occurring less frequently (Figure 5L–N and Supplemental Video S2). It is important to point out that cytokinesis in the dental epithelium often happen quickly, within 5–10 min. As a result, timelapse intervals of more than 5 min may miss some of these divisions.

Cell division events were also apparent in *K14*^{Cre};*R26*$^{mT/mG}$ cervical loops, where all epithelial cell membranes were labelled green (Figure 6A). We could identify mitotic cells by their cell rounding and then cytokinesis (Supplemental Video S3), and both vertical and horizontal cell divisions were observable (Figure 6B–G), thus similar to the results obtained using H2B-GFP. Together, these results demonstrate that this protocol can serve as a powerful tool to investigate cell behaviors in the incisor explants when combined with mouse genetic models that fluorescently label distinct subcellular structures.

DISCUSSION:

Live tissue imaging is an important technique that allows us to study the dynamic processes and behaviors of cells when they are maintained in their niche environment[41]. Ideally, live imaging is performed *in vivo* with high spatiotemporal resolution. However, *in vivo* imaging for mammalian organs can be challenging due to tissue inaccessibility, optical opaqueness, and difficulty of immobilizing the animal or the organ for a prolonged period[42]. Tissue explants bypass some of these challenges and have been successfully adopted in a number of studies to track cell behaviors, such as during tooth morphogenesis and development

of ectodermal organs[26]. Here, we demonstrated a relatively simple yet robust protocol to perform live deep tissue imaging on cultured whole adult mouse incisors. Application of this technique will help us understand the regulation of cell movements, fate decisions, and tissue organizations during dental regeneration.

Because cell divisions are easily observable events and characteristic of regenerating tissues, we have focused on tracking dividing cells in this study to highlight one usage of the protocol. We found that incisor epithelial progenitors can undergo both vertical and horizontal divisions, thus similar to other epithelial tissues[43]. Elucidating the mechanism that regulates division angles and investigating the role of division orientations in cell fate decisions will be of importance in future studies. Combining live imaging with different mouse genetic models that also carry fluorescent cell fate markers, signaling pathway reporters, or the Fucci cell cycle reporter[44, 45] will help unveil how cell division patterns and cell cycle dynamics contribute to the regulation of epithelial homeostasis and regeneration.

A necessary practice in this protocol is to carry out tooth dissection in an expeditious and careful manner, allowing quick transition to and preservation of the intact tissue under the appropriate culturing condition. We have found that for live imaging, dissecting tissues in warm media, rather than cold media, as in experiments aimed to extract proteins and mRNAs[46], maintains cells in a functioning state. Because the incisor is a relatively large organ for culturing, a steady supply of nutrients via media perfusion is also critical for the sustainment of the tissue throughout imaging[47]. If the progenitor cells are present in the region of interest, observation of frequent cell divisions is a good indicator that the tissue is healthy and active. In contrast, cell death should be infrequent, and this can be verified by detecting bright and condensed nuclear bodies during imaging if a nuclear marker is used or by performing TUNEL staining after imaging and tissue fixation[48]. In addition to nutrients, oxygen levels may also affect explant viability, as either oxygen tension or insufficiency can disrupt cell survival, proliferation, and differentiation[49–51]. In our experience, we have not observed apparent differences in cell proliferation and cell death when samples were provided with or without additional oxygen (e.g. 95% O_2/5% CO_2 carbogen or 5% CO_2/21% O_2/balanced N_2) during imaging, suggesting that either trace amount of oxygen in the system is sufficient to maintain incisor epithelia in culture overnight or the tissue can employ alternative pathways to maintain normal cell functions[52]. However, the requirement for oxygen in other cellular processes or correct gene expression should be further determined in future studies.

In our demonstration of the protocol, we have used genetically encoded H2BGFP and membrane GFP to label cell nuclei and contours, respectively. These fluorescent markers are bright and long-lasting under two-photon microscopy and are thus examples of ideal labels to use for tracking cell movements and divisions. In theory, fluorescent vital dyes can also be used to label different subcellular compartments for *ex vivo* live imaging[53], but reduced penetration of the dyes into deeper epithelial cells likely limits their uses. Similarly, while standard confocal microscopy is capable of high-resolution live imaging at a depth under 100 μm, two-photon microscopy provides increased imaging depth with reduced photobleaching and phototoxicity[54]. We have therefore chosen two-photon microscopy as an imaging modality in most of our live imaging applications.

One potential limitation of this protocol is that incisor explants may not fully recapitulate the *in vivo* environment and biology. Data therefore represent cell behaviors under the culture condition and should be interpreted accordingly as well as validated using other methods, such as histology, when applicable. We also had to partially remove periodontal tissues to gain access to the cervical loop for imaging. Signaling interactions between periodontal tissues and the dental epithelium could thus be disrupted. Lastly, while media perfusion greatly improves the viability of cultured tissues, it could introduce fluid shear stress that acts as an ectopic mechanical signal and affects results[55, 56]. We have not determined the impact of different flow rates in our setup. However, because a low flow rate at 1–5 mL/h is typically sufficient for maintaining nutrient supplies[57], the effect of shear stress can be minimized. With these limitations in mind, *ex vivo* live imaging serves as a powerful platform to study changes in cell behaviors when the appropriate controls are included in experiments.

The continuously growing mouse incisor is a highly tractable model system to study stem cell-based tissue renewal and injury repair. The protocol described herein provides investigators with the means to maintain whole adult incisors in culture and extract spatiotemporal information about cell behaviors through timelapse microscopy. We expect this technique to be broadly applicable to studying different mouse genetic models used in dental research and to help advance our knowledge in the field of dental regeneration.

Supplementary Material

Refer to Web version on PubMed Central for supplementary material.

ACKNOWLEDGMENTS:

We acknowledge the UCLA Advanced Light Microscopy/Spectroscopy Laboratory and Leica Microsystems Center of Excellence at the California NanoSystems Institute (RRID:SCR_022789) for providing two-photon microscopy. AS was supported by ISF 604-21 from the Israel Science Foundation. JH was supported by R03DE030205 and R01DE030471 from the NIH/NIDCR. AS and JH were also supported by grant 2021007 from the United States-Israel Binational Science Foundation (BSF).

REFERENCES:

1. Yu T, Volponi AA, Babb R, An Z, Sharpe PT Stem Cells in Tooth Development, Growth, Repair, and Regeneration. Current Topics in Developmental Biology. 115, 187–212, doi: 10.1016/bs.ctdb.2015.07.010 (2015). [PubMed: 26589926]
2. Jing J, Zhang M, Guo T, Pei F, Yang Y, Chai Y Rodent incisor as a model to study mesenchymal stem cells in tissue homeostasis and repair. Frontiers in Dental Medicine. 3 (2022).
3. Harada H, Kettunen P, Jung H-S, Mustonen T, Wang YA, Thesleff I Localization of Putative Stem Cells in Dental Epithelium and Their Association with Notch and Fgf Signaling. Journal of Cell Biology. 147 (1), 105–120, doi: 10.1083/jcb.147.1.105 (1999). [PubMed: 10508859]
4. Warshawsky H, Smith CE Morphological classification of rat incisor ameloblasts. The Anatomical Record. 179 (4), 423–445, doi: 10.1002/ar.1091790403 (1974). [PubMed: 4135484]
5. Lekic P, McCulloch CA Periodontal ligament cell population: the central role of fibroblasts in creating a unique tissue. The Anatomical Record. 245 (2), 327–341, doi: 10.1002/(SICI)1097-0185(199606)245:2<327::AID-AR15>3.0.CO;2-R (1996). [PubMed: 8769671]
6. Takahashi A et al. Autocrine regulation of mesenchymal progenitor cell fates orchestrates tooth eruption. Proceedings of the National Academy of Sciences. 116 (2), 575–580, doi: 10.1073/pnas.1810200115 (2019).

7. Ness AR Eruption rates of impeded and unimpeded mandibular incisors of the adult laboratory mouse. Archives of Oral Biology. 10 (3), 439–451, doi: 10.1016/0003-9969(65)90109-3 (1965). [PubMed: 5231526]
8. Smith CE, Warshawsky H Cellular renewal in the enamel organ and the odontoblast layer of the rat incisor as followed by radioautography using 3H-thymidine. The Anatomical Record. 183 (4), 523–561, doi: 10.1002/ar.1091830405 (1975). [PubMed: 1200409]
9. Seidel K et al. Hedgehog signaling regulates the generation of ameloblast progenitors in the continuously growing mouse incisor. Development (Cambridge, England). 137 (22), 3753–3761, doi: 10.1242/dev.056358 (2010). [PubMed: 20978073]
10. Juuri E et al. Sox2+ stem cells contribute to all epithelial lineages of the tooth via Sfrp5+ progenitors. Developmental Cell. 23 (2), 317–328, doi: 10.1016/j.devcel.2012.05.012 (2012). [PubMed: 22819339]
11. Biehs B et al. BMI1 represses Ink4a/Arf and Hox genes to regulate stem cells in the rodent incisor. Nature Cell Biology. 15, 846–852, doi: 10.1038/ncb2766 (2013). [PubMed: 23728424]
12. Feng J, Mantesso A, De Bari C, Nishiyama A, Sharpe PT Dual origin of mesenchymal stem cells contributing to organ growth and repair. Proceedings of the National Academy of Sciences of the United States of America. 108 (16), 6503–6508, doi: 10.1073/pnas.1015449108 (2011). [PubMed: 21464310]
13. Zhao H et al. Secretion of shh by a neurovascular bundle niche supports mesenchymal stem cell homeostasis in the adult mouse incisor. Cell Stem Cell. 14 (2), 160–173, doi: 10.1016/j.stem.2013.12.013 (2014). [PubMed: 24506883]
14. Li L, Clevers H Coexistence of Quiescent and Active Adult Stem Cells in Mammals. Science. 327 (5965), 542–545, doi: 10.1126/science.1180794 (2010). [PubMed: 20110496]
15. Sharir A et al. A large pool of actively cycling progenitors orchestrates self-renewal and injury repair of an ectodermal appendage. Nature Cell Biology. 21 (9), 1102–1112, doi: 10.1038/s41556-019-0378-2 (2019). [PubMed: 31481792]
16. Hu JK-H, Du W, Shelton SJ, Oldham MC, DiPersio CM, Klein OD An FAK-YAP-mTOR Signaling Axis Regulates Stem Cell-Based Tissue Renewal in Mice. Cell Stem Cell. 21 (1), 91–106.e6, doi: 10.1016/j.stem.2017.03.023 (2017). [PubMed: 28457749]
17. Yu F, Li F, Zheng L, Ye L Epigenetic controls of Sonic hedgehog guarantee fidelity of epithelial adult stem cells trajectory in regeneration. Science Advances. 8 (29), eabn4977, doi: 10.1126/sciadv.abn4977 (2022).
18. An Z, Sabalic M, Bloomquist RF, Fowler TE, Streelman T, Sharpe PT A quiescent cell population replenishes mesenchymal stem cells to drive accelerated growth in mouse incisors. Nature Communications. 9 (1), 378, doi: 10.1038/s41467-017-02785-6 (2018).
19. Balic A, Thesleff I Tissue Interactions Regulating Tooth Development and Renewal. Current Topics in Developmental Biology. 115, 157–186, doi: 10.1016/bs.ctdb.2015.07.006 (2015). [PubMed: 26589925]
20. Yu T, Klein OD Molecular and cellular mechanisms of tooth development, homeostasis and repair. Development. 147 (2), doi: 10.1242/dev.184754 (2020).
21. Krivanek J, Buchtova M, Fried K, Adameyko I Plasticity of Dental Cell Types in Development, Regeneration, and Evolution. Journal of Dental Research. 102 (6), 589–598, doi: 10.1177/00220345231154800 (2023). [PubMed: 36919873]
22. Helmchen F, Denk W Deep tissue two-photon microscopy. Nature Methods. 2 (12), 932–940, doi: 10.1038/nmeth818 (2005). [PubMed: 16299478]
23. Cetera M, Leybova L, Joyce B, Devenport D Counter-rotational cell flows drive morphological and cell fate asymmetries in mammalian hair follicles. Nature Cell Biology. 20 (5), 541–552, doi: 10.1038/s41556-018-0082-7 (2018). [PubMed: 29662173]
24. Held M, Santeramo I, Wilm B, Murray P, Lévy R Ex vivo live cell tracking in kidney organoids using light sheet fluorescence microscopy. PLoS ONE. 13 (7), e0199918, doi: 10.1371/journal.pone.0199918 (2018). [PubMed: 30048451]
25. Mesa KR et al. Homeostatic Epidermal Stem Cell Self-Renewal Is Driven by Local Differentiation. Cell Stem Cell. 23 (5), 677–686.e4, doi: 10.1016/j.stem.2018.09.005 (2018). [PubMed: 30269903]

26. Mogollón I, Ahtiainen L Live Tissue Imaging Sheds Light on Cell Level Events During Ectodermal Organ Development. Frontiers in Physiology. 11, 818, doi: 10.3389/fphys.2020.00818 (2020). [PubMed: 32765297]
27. Prochazka J et al. Migration of Founder Epithelial Cells Drives Proper Molar Tooth Positioning and Morphogenesis. Developmental Cell. 35 (6), 713–724, doi: 10.1016/j.devcel.2015.11.025 (2015). [PubMed: 26702830]
28. Morita R et al. Coordination of Cellular Dynamics Contributes to Tooth Epithelium Deformations. PLOS ONE. 11 (9), e0161336, doi: 10.1371/journal.pone.0161336 (2016). [PubMed: 27588418]
29. Ahtiainen L, Uski I, Thesleff I, Mikkola ML Early epithelial signaling center governs tooth budding morphogenesis. The Journal of Cell Biology. 214 (6), 753–767, doi: 10.1083/jcb.201512074 (2016). [PubMed: 27621364]
30. Panousopoulou E, Green JBA Invagination of Ectodermal Placodes Is Driven by Cell Intercalation-Mediated Contraction of the Suprabasal Tissue Canopy. PLoS biology. 14 (3), e1002405, doi: 10.1371/journal.pbio.1002405 (2016). [PubMed: 26960155]
31. Mogollón I, Moustakas-Verho JE, Niittykoski M, Ahtiainen L The initiation knot is a signaling center required for molar tooth development. Development. 148 (9), dev194597, doi: 10.1242/dev.194597 (2021).
32. Kim R et al. Early perturbation of Wnt signaling reveals patterning and invagination-evagination control points in molar tooth development. Development. 148 (14), dev199685, doi: 10.1242/dev.199685 (2021).
33. Takahashi M, Makino S, Kikkawa T, Osumi N Preparation of Rat Serum Suitable for Mammalian Whole Embryo Culture. Journal of Visualized Experiments : JoVE. (90), 51969, doi: 10.3791/51969 (2014). [PubMed: 25145996]
34. Katsuragi Y et al. Bcl11b transcription factor plays a role in the maintenance of the ameloblast-progenitors in mouse adult maxillary incisors. Mechanisms of Development. 130 (9–10), 482–492, doi: 10.1016/j.mod.2013.05.002 (2013). [PubMed: 23727454]
35. Dassule HR, Lewis P, Bei M, Maas R, McMahon AP Sonic hedgehog regulates growth and morphogenesis of the tooth. Development. 127 (22), 4775–4785 (2000). [PubMed: 11044393]
36. Belteki G et al. Conditional and inducible transgene expression in mice through the combinatorial use of Cre-mediated recombination and tetracycline induction. Nucleic Acids Research. 33 (5), e51, doi: 10.1093/nar/gni051 (2005). [PubMed: 15784609]
37. Tumbar T et al. Defining the epithelial stem cell niche in skin. Science. 303 (5656), 359–363, doi: 10.1126/science.1092436 (2004). [PubMed: 14671312]
38. Muzumdar MD, Tasic B, Miyamichi K, Li L, Luo L A global double-fluorescent Cre reporter mouse. Genesis. 45 (9), 593–605, doi: 10.1002/dvg.20335 (2007). [PubMed: 17868096]
39. Kimura H, Cook PR Kinetics of Core Histones in Living Human Cells. The Journal of Cell Biology. 153 (7), 1341–1354 (2001). [PubMed: 11425866]
40. Kanda T, Sullivan KF, Wahl GM Histone-GFP fusion protein enables sensitive analysis of chromosome dynamics in living mammalian cells. Current biology: CB. 8 (7), 377–385, doi: 10.1016/s0960-9822(98)70156-3 (1998). [PubMed: 9545195]
41. Huang Q et al. The frontier of live tissue imaging across space and time. Cell Stem Cell. 28 (4), 603–622, doi: 10.1016/j.stem.2021.02.010 (2021). [PubMed: 33798422]
42. Skylaki S, Hilsenbeck O, Schroeder T Challenges in long-term imaging and quantification of single-cell dynamics. Nature Biotechnology. 34 (11), 1137–1144, doi: 10.1038/nbt.3713 (2016).
43. Knoblich JA Mechanisms of Asymmetric Stem Cell Division. Cell. 132 (4), 583–597, doi: 10.1016/j.cell.2008.02.007 (2008). [PubMed: 18295577]
44. Li S et al. Overview of the reporter genes and reporter mouse models. Animal Models and Experimental Medicine. 1 (1), 29–35, doi: 10.1002/ame2.12008 (2018). [PubMed: 30891544]
45. Mort RL et al. Fucci2a: a bicistronic cell cycle reporter that allows Cre mediated tissue specific expression in mice. Cell Cycle. 13 (17), 2681–2696, doi: 10.4161/15384101.2015.945381 (2014). [PubMed: 25486356]
46. Krivanek J et al. Dental cell type atlas reveals stem and differentiated cell types in mouse and human teeth. Nature Communications. 11 (1), 4816, doi: 10.1038/s41467-020-18512-7 (2020).

47. Dailey ME, Marrs GS, Kurpius D Maintaining Live Cells and Tissue Slices in the Imaging Setup. Cold Spring Harbor protocols. 2011 (4), pdb.top105 (2011).

48. Gorczyca W, Bruno S, Darzynkiewicz R, Gong J, Darzynkiewicz Z DNA strand breaks occurring during apoptosis - their early insitu detection by the terminal deoxynucleotidyl transferase and nick translation assays and prevention by serine protease inhibitors. International Journal of Oncology. 1 (6), 639–648, doi: 10.3892/ijo.1.6.639 (1992). [PubMed: 21584593]

49. Aguilera-Castrejon A et al. Ex utero mouse embryogenesis from pre-gastrulation to late organogenesis. Nature. 593 (7857), 119–124, doi: 10.1038/s41586-021-03416-3 (2021). [PubMed: 33731940]

50. Wale PL, Gardner DK Time-lapse analysis of mouse embryo development in oxygen gradients. Reproductive Biomedicine Online. 21 (3), 402–410, doi: 10.1016/j.rbmo.2010.04.028 (2010). [PubMed: 20691637]

51. Tse HM, Gardner G, Dominguez-Bendala J, Fraker CA The Importance of Proper Oxygenation in 3D Culture. Frontiers in Bioengineering and Biotechnology. 9 (2021).

52. Spinelli JB et al. Fumarate is a terminal electron acceptor in the mammalian electron transport chain. Science. 374 (6572), 1227–1237, doi: 10.1126/science.abi7495 (2021). [PubMed: 34855504]

53. Johnson S, Rabinovitch P Ex-vivo imaging of excised tissue using vital dyes and confocal microscopy. Current Protocols in Cytometry. CHAPTER, Unit9.39, doi: 10.1002/0471142956.cy0939s61 (2012).

54. Combs CA, Shroff H Fluorescence Microscopy: A Concise Guide to Current Imaging Methods. Current Protocols in Neuroscience. 79, 2.1.1–2.1.25, doi: 10.1002/cpns.29 (2017).

55. McCoy RJ, O'Brien FJ Influence of shear stress in perfusion bioreactor cultures for the development of three-dimensional bone tissue constructs: a review. Tissue Engineering. Part B, Reviews. 16 (6), 587–601, doi: 10.1089/ten.TEB.2010.0370 (2010). [PubMed: 20799909]

56. Chen KD et al. Mechanotransduction in response to shear stress. Roles of receptor tyrosine kinases, integrins, and Shc. The Journal of Biological Chemistry. 274 (26), 18393–18400, doi: 10.1074/jbc.274.26.18393 (1999). [PubMed: 10373445]

57. Seddiqi H et al. Inlet flow rate of perfusion bioreactors affects fluid flow dynamics, but not oxygen concentration in 3D-printed scaffolds for bone tissue engineering: Computational analysis and experimental validation. Computers in Biology and Medicine. 124, 103826, doi: 10.1016/j.compbiomed.2020.103826 (2020). [PubMed: 32798924]

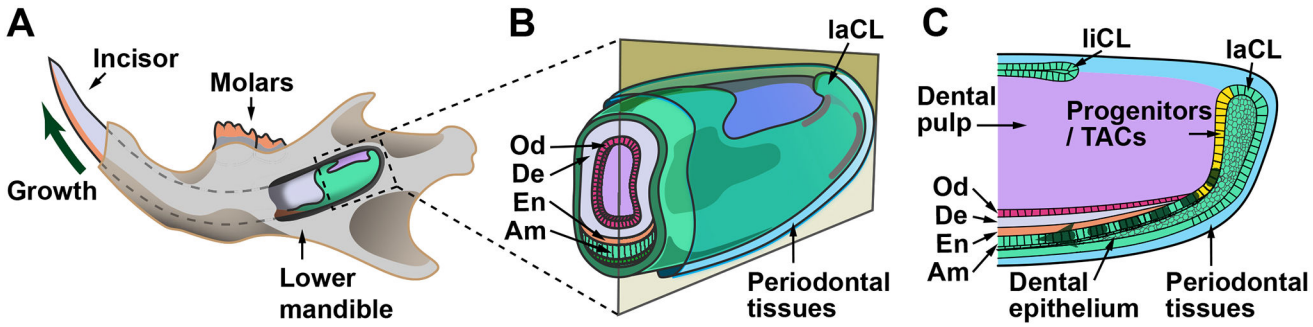

Figure 1: Schematics of the mouse jaw and incisor cervical loop.

(**A**) A significant portion of the incisor is embedded in the jawbone. The growth region is located at the apical end of the tooth and supports its continuous growth (dark green arrow). (**B**) An enlargement of the apical incisor, which is surrounded by periodontal tissues. The tooth is composed of enamel and dentin, which are highly mineralized structures formed by ameloblasts and odontoblasts, respectively. (**C**) A sagittal section of the apical incisor, showing that dental epithelial progenitor cells and transit-amplifying cells reside in the labial cervical loop and give rise to ameloblasts in the more distal epithelium (dark green dashed arrow). Compared to the labial cervical loop, the lingual cervical loop is smaller in size and does not normally form ameloblasts. Dental mesenchymal stem cells are present in the dental pulp (purple region) and give rise to odontoblasts. Abbreviations: En = enamel; De = dentin; Am = ameloblast; Od = odontoblast; TACs = transit-amplifying cells; laCL = labial cervical loop; liCL = lingual cervical loop.

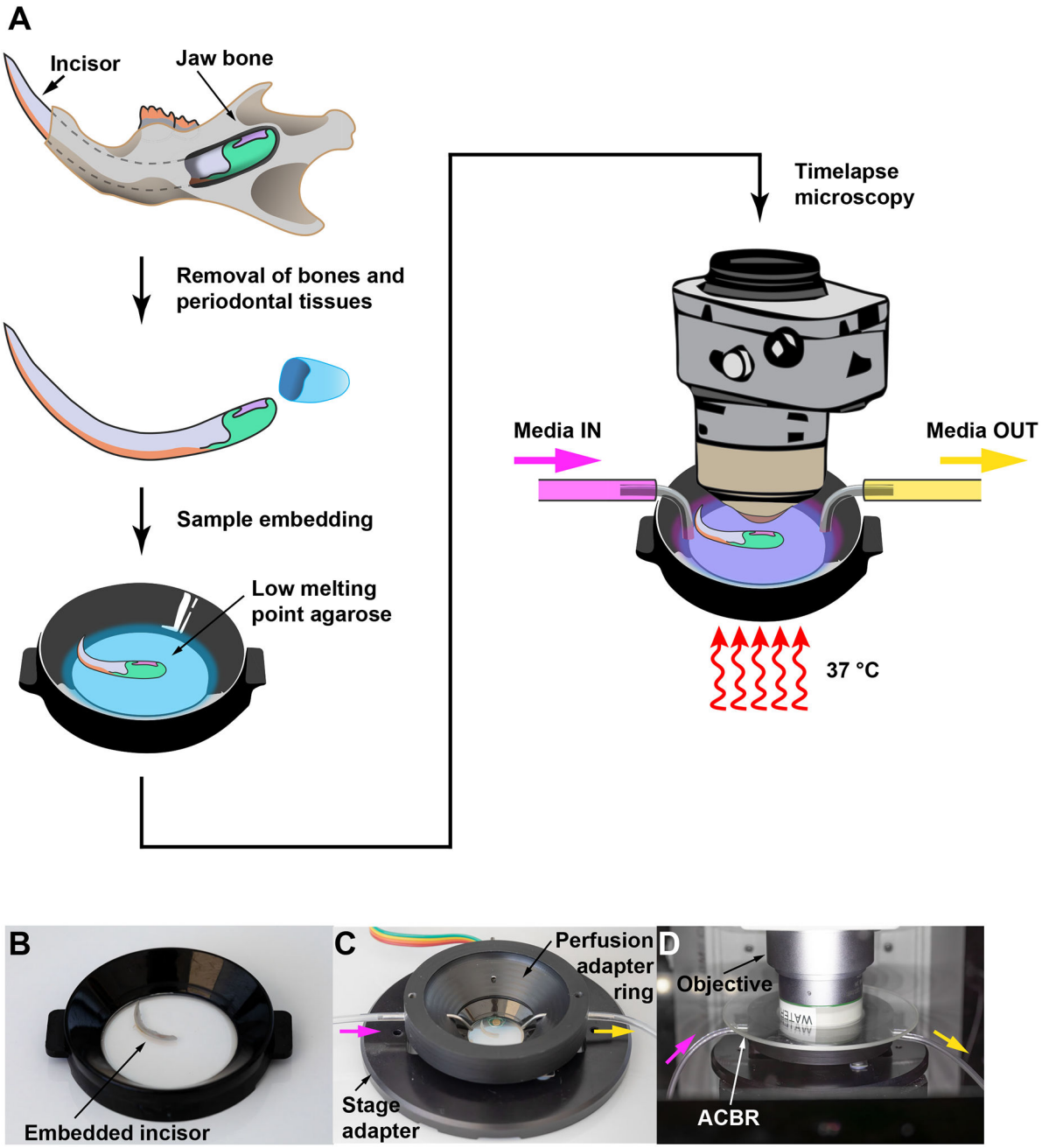

Figure 2: Maintaining mouse incisor explant for live imaging.

(**A**) A schematic depicting key steps of the protocol, from dissecting the incisor to embedding the tissue in low melting point agarose for live imaging. A perfusion setup is used to provide a constant supply of nutrients during imaging. (**B–D**) A step-by-step demonstration of setting the culture dish and the perfusion chamber for live imaging. Media inlet and outlet are shown as pink and yellow arrows respectively. Abbreviation: ACBR = Atmospheric Control Barrier Ring.

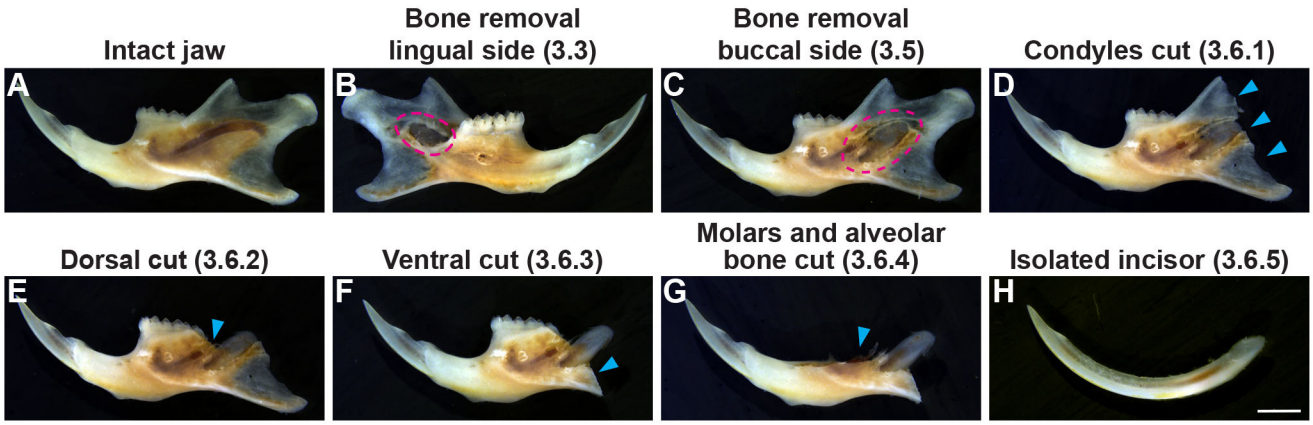

Figure 3: Isolation of the whole mouse incisor.

(**A**) Intact jaw. (**B–H**) Bones were gradually removed to expose the whole incisor. Red dashed lines in B and C show the exposed soft tissue of the apical incisor after shaving off the membrane bone overlying the lingual and buccal sides of the incisor socket (steps 3.3–3.5 in the protocol). (**D–G**) Blue arrowheads represent the condyles, molars, and alveolar bones that have been removed to isolate the entire tooth (step 3.6 in the protocol). Scale bar = 2 mm (**H**).

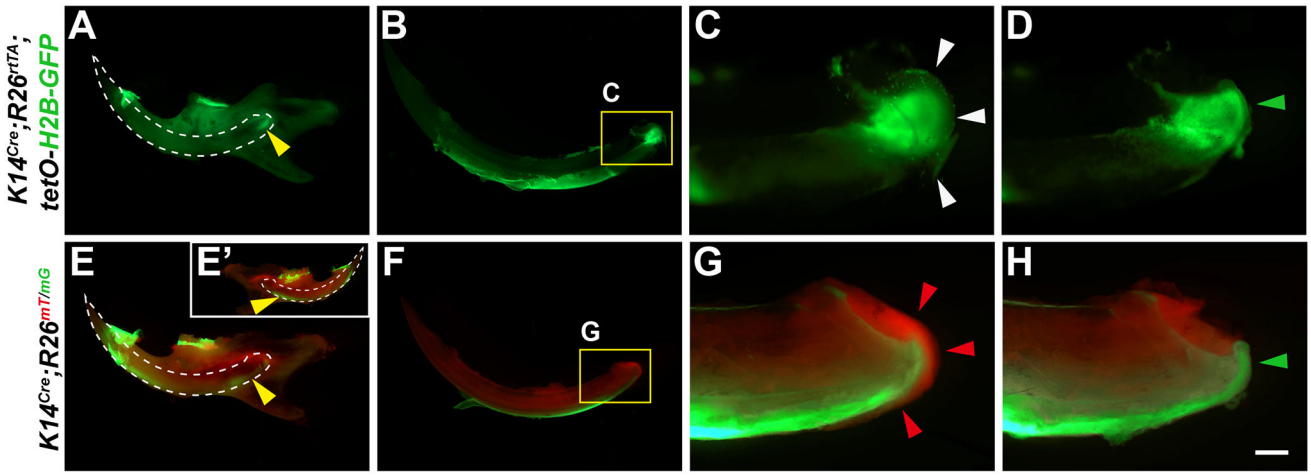

Figure 4: Removal of periodontal tissues for live imaging.

(**A–H**) Representative samples from (**A–D**) *K14*^{Cre};*R26*^{rtTA};*tetO-H2B-GFP*, and (**E–H**) *K14*^{Cre};*R26*$^{mT/mG}$ mice were used in our demonstration of the protocol. Before dissection, GFP expression in the dental epithelium was visible through the bone (**A,E**, yellow arrowheads). White dashed lines outline the undissected incisors. **E'** shows the lingual side. In isolated incisors (**B,C,F,G**), GFP fluorescence was initially diffracted by the periodontal tissues covering the apical incisors (white and red arrowheads). Red fluorescence in **F** and **G** labels non-epithelial cells. Removal of periodontal tissues allows clear and unobstructed view of the green fluorescent cervical loops (**D**,**H**, green arrowheads). Scale bar = 2 mm (**A,E**); 1.25 mm (**B,F**); and 300 μm (**C,D,G,H**).

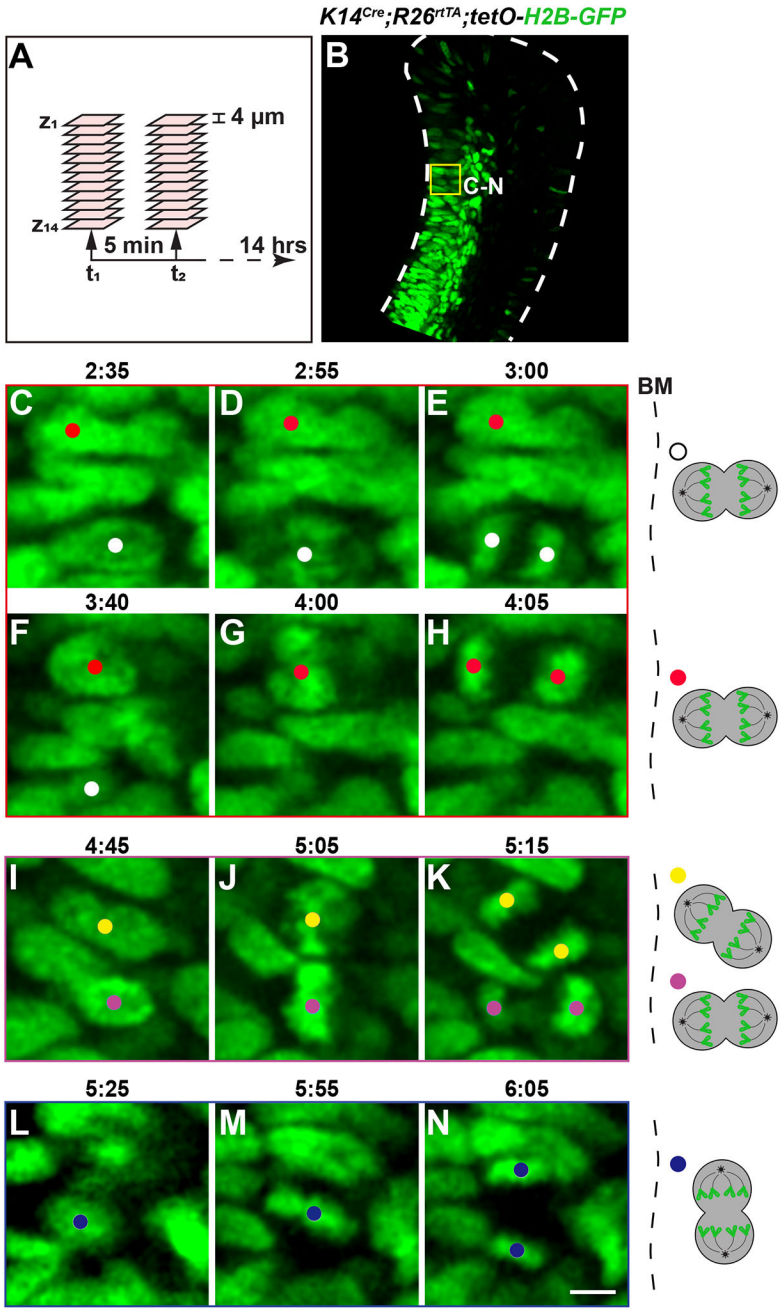

Figure 5: Timelapse microscopy of the *K14*^{Cre};*R26*^{rtTA};*tetO-H2B-GFP* cervical loop.

(**A**) A schematic illustrating the timelapse setup. (**B**) A representative z-plane of the *K14*^{Cre};*R26*^{rtTA};*tetO-H2B-GFP* incisor labial cervical loop, showing nuclear labelling by H2B-GFP primarily in the transit-amplifying region, where cells actively divide. Yellow box represents the general area of the enlarged images shown below. (**C–K**) Timelapse images showing vertical and oblique cell divisions relative to the BM. (**L–N**) Timelapse images showing an example of horizontal cell division relative to the BM. (**D,G,J,M**) Cells in metaphase or anaphase are displayed in the middle panels. Schematics of each tracked

division are shown on the right. Scale bar in N = 36 μm (**B**); 5 μm (**C–N**). Abbreviation: BM = basement membrane.

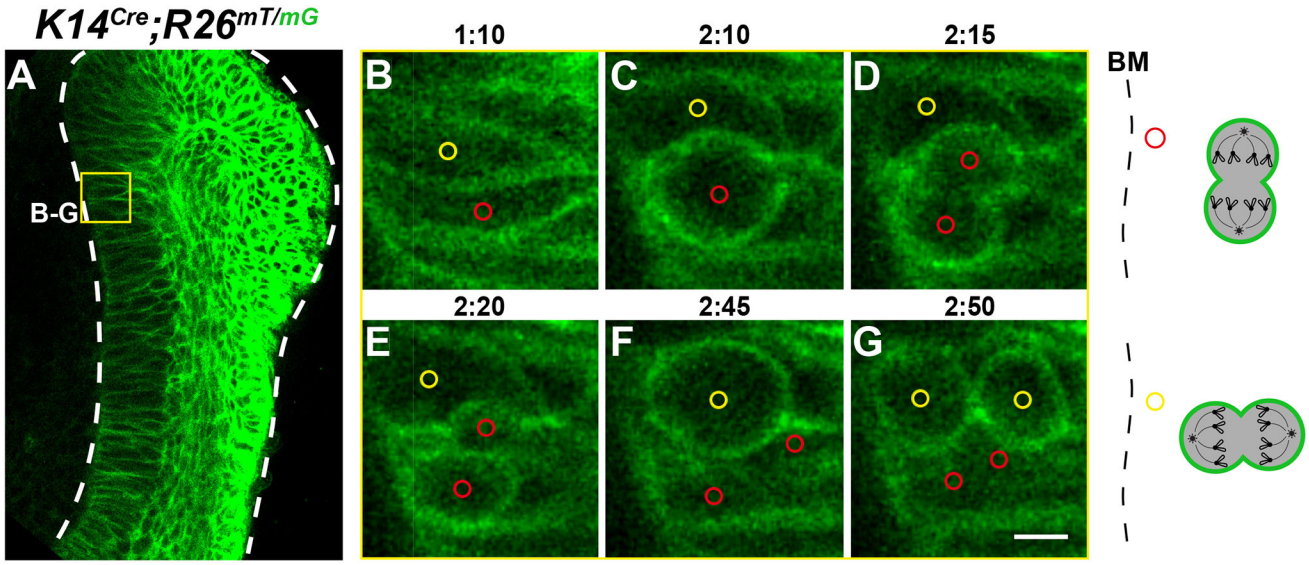

Figure 6: Timelapse microscopy of the *K14*^{Cre};*R26*$^{mT/mG}$ cervical loop.

(**A**) A representative z-plane of the *K14*^{Cre};*R26*$^{mT/mG}$ incisor labial cervical loop. All epithelial cells express membrane GFP. Yellow box represents the area of cell tracking shown in the enlargements. (**B–G**) Timelapse images capturing both (**B–D**) horizontal and (**E–G**) vertical cell divisions, relative to the BM. (**C,F**) Middle panels show mitotic cell rounding. Schematics of each tracked division are shown on the right. Scale bar = 35 μm (**A**); 5 μm (**B–G**). Abbreviation: BM = basement membrane.

Table of Materials

Name of Material/ Equipment	Company	Catalog Number	Comments/Description
24 well, flat bottom tissue culture plate	Olympus plastics	25-107	
25x HC IRAPO motCORR water dipping objective	Leica	11507704	
Ascorbic acid (Vitamin C)	Acros Organics	352685000	
D-(+)-Glucose bioxtra	Sigma Aldrich	G7528	
Delta T system	Bioptechs	0420-4	Including temperature control, culture dishes, and perfusion setup
Dissection microscope- LEICA S9E	Leica	LED300 SLI	
DMEM/F12	Thermo Scientific	11039047	Basal media without phenol red
Feather surgical blade (#15)	Feather	72044-15	
Fine forceps	F.S.T	11252-23	
Glutamax	Thermo Scientific	35050-061	Glutamine substitute
Leica SP8-DIVE equipped with a 25X HC IRAPO motCORR water dipping objective	Leica	n/a	
low-melting agarose	NuSieve	50080	
non-essential amino acids (100X)	Thermo Scientific	11140-050	
penicillin–streptomycin	Thermo Scientific	15140122	10,000 U/mL
Petri dish	Gen Clone	32-107G	90 mm
Rat serum	Valley Biomedical	AS3061SC	Processed for live imaging
Razor blade #9	VWR	55411-050	
Scalpel handle	F.S.T	10003-12	
Scissors	F.S.T	37133	
serrated forceps	F.S.T	11000-13	
spring scissors	F.S.T	91500-09	